EUCLIPSE

EU Cloud Intercomparison, Process Study & Evaluation Project

Grant agreement no. 244067

Deliverable D2.4 – ESM evaluation of the ITCZ, the intra-seasonal and inter-annual variability of the tropical atmosphere and temperature extremes over Europe.

Delivery date: 24 months

EUCLIPSE WP2 Deliverable D2.4:

Ability of climat models to simulate the ITCZ, the intra-seasonal and inter-annual variability of the tropical atmosphere, and temperature extremes over Europe using a new set of diagnostics

Main contributors to this report:
Gilles Bellon and Boutheina Oueslati, CNRS/CNRM/Meteo-France (section 1)
Hugo Bellenger and Eric Guilyardi, CNRS/LOCEAN/IPSL (section 2)
Julien Cattiaux and Hervé Douvile, CNRS/CNRM/Meteo-France (section 3)

WP2 coordinator:
Sandrine Bony (CNRS/LMD/IPSL)

January 2012

WP2 is focused on the analysis and the evaluation of climate simulations from CMIP5 (the 5th Phase of the Coupled Models Intercomparison Project), and the Task 2 of this WP aims at understanding how cloud and moist processes affect the simulation of the tropical atmosphere and temperature extremes in the current climate. This report presents an early analysis of the ability of CMIP5 climate models to simulate the Inter-Tropical Convergence Zone (ITCZ) and the Madden-Julian Oscillations (MJO, section 1), the tropical inter-annual variability (the El-Niño Southern Oscillation or ENSO, section 2), and temperature extremes over Europe (section 3). Climate model outputs have been available on the CMIP5 data archive (Earth System Grid) later than anticipated at the time of the writing of the EUCLIPSE proposal. For this reason, the focus of this deliverable is put on the evaluation of a subset of CMIP5 models, especially those developped by EUCLIPSE participants (CNRM-CM5, HadGEM2, IPSL-CM5A, MPI-ESM; unfortunately, EC-Earth and IPSL-CM5B outputs are not yet available for analysis). By the end of the project, additional models will be considered, and the role of the representation of cloud and moist processes in the models' ability to reproduce the observed tropical variability and european extremes will be examined in more details.

1 ITCZ and MJO in the CMIP5 models

Some of the models show some improvement in the simulation of the seasonal and intraseasonal variability of tropical precipitation. The double ITCZ bias is still present in most of the models. This bias is reduced in most models participating to EUCLIPSE compared to the previous generations of the same models. In particular, it appears that the double ITCZ bias has become small in atmosphere-only simulations, and that coupled feedbacks account for a large part of this bias in coupled simulations. Some improvement can be found in the simulation of intraseasonal variability, in particular in models whose previous generation already performed better. Among these models, the role of the ocean-atmosphere coupling seems to be quite different from one model to the other.

1.1 Seasonal cycle of the precipitation

Figure 1 shows the annual average of precipitation in the ocean-atmosphere models participating to EUCLIPSE. Most of the models simulate too strong oceanic ITCZs. All of them also exhibit the well-known double-ITCZ bias,

with a spurious longitudinal rainband south of the equator in the East Pacific. Some also simulate a double ITCZ in the tropical Atlantic.

But except for the HadGEM-ES model, all the models participating to EUCLIPSE reduced their double ITCZ biases compared to the previous version ,as shown in Figure 2 by a metric proposed by Bellucci et al. (2010), the Southern ITCZ index (average annual precipitation between 100W and 150W, 0 and 20S).

Indeed, the seasonal cycle of the precipitation in the East Pacific (80W-120W) has improved in coupled models, as shown in Figure 3, compared to Dai (2006) and de Szoeke and Xie (2008). In particular, the CNRM-CM5 no longer simulates a double ITCZ all year round, but simulates a single ITCZ that moves accross the equator following the solar forcing, similarly to the IPSL-CM5A and MPI-ESM. Only the HadGEM-ES simulates the observed March-April double ITCZ but the Southern ITCZ is then much more intense than in the observations (the increase of the SI index from CMIP3 to CMIP5 is actually due to this enhanced precipitation).

Figure 4 shows the seasonal cycle of precipitation in the East Pacific in the atmosphere-only simulations. Compared to the ocean-atmosphere coupled simulations, the precipitation biases are much reduced, and the biases of the atmospheric models do not easily relate to those of the coupled models. In the East Pacific, the MPI model ECHAM and the CNRM model ARPEGE even underestimate the precipitation in the March/April Southern ITCZ. It shows that the coupled ocean-atmosphere feedbacks are responsible for most of the double ITCZ bias in the East Pacific, maybe more so than in the previous generation of models (Lin 2007). Coupled feedbacks are also essential in modulating the double ITCZ bias, and they are responsible for a large part of the inter-model differences.

1.2 Intraseasonal variability

Figure 5 shows the symmetric and asymmetric (with respect to the equator), space and time cross-spectra of tropical OLR and zonal wind at 850 hPa, that is a classical diagnosis of subseasonal tropical variability (see Wheeler and Kiladis 1999). The Madden Julian Oscillation appears as a maximum of the symmetric spectrum between wavenumbers 1 and 2, in the 30-50-day range. Eastward-propagating (positive wavenumbers) Kelvin waves appear in the symmetric spectrum along the straight lines, while westward-propagating (negative wavenumbers) Equatorial Rossby waves appear on the same spectrum in the 10-80-day range. Mixed Rossby-Gravity wave can be seen in the center of the asymmetric spectrum.

The CMIP5 models exhibit contrasting skills at simulating the subseasonal variabilit. The IPSL-CM5A simulates a very weak subseasonal variability. The CNRM-CM5 exhibits subseasonal variability close to the observation in terms of power, but the dispersion of gravity (Kelvin and Mixed Rossby-Gravity) waves differs from the observations. It corresponds to a deeper equivalent depth of the troposphere in that model. The MPI-ESM simulates a very realistic subseasonal variability, but with underestimated power (recent analyses suggest that the OLR variation on intraseasonal scales in this model is not simulated with a consistent phase with respect to the wind and precipitation signals, reducing the cross-spectrum power). The MPI and CNRM models simulate an MJO varaibility that is enhanced, closer to the observed intensity compared to the previous generation of models (Lin et al. 2006). In the previous generation of models, the IPSL model simulated more kelvin-wave variability, and the CNRM model did not simulate much of these waves. The MPI model kept most of the characteristics of the previous generation.

The contrast between coupled models is even more pronounced in terms of the role of the ocean-atmosphere coupling. Figure 6 shows the same spectra as in figure 5, but for the corresponding atmosphere-only models. The coupling clearly enhances the MJO in all the models, but much more so in CNRM-CM5 than in the MPI-ESM. The convectively-coupled gravity waves are fairly insensitive to the coupling, except maybe in the IPSL-CM5A model in

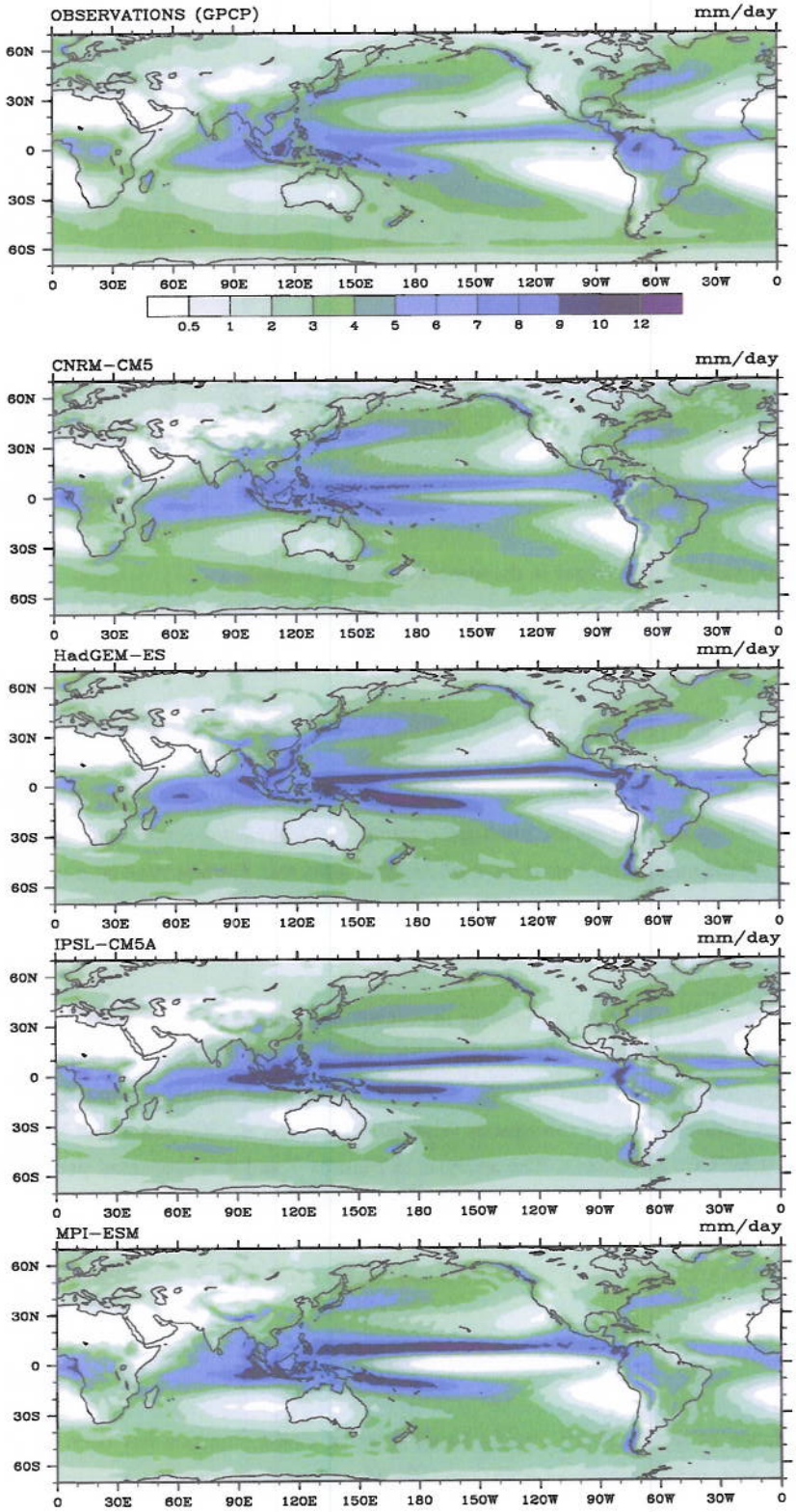

Figure 1: Mean annual precipitation as observed (GPCP) and simulated by some CMIP5 models (CNRM-CM5, HadGEM-ES, IPSL-CM5A, MPI-ESM).

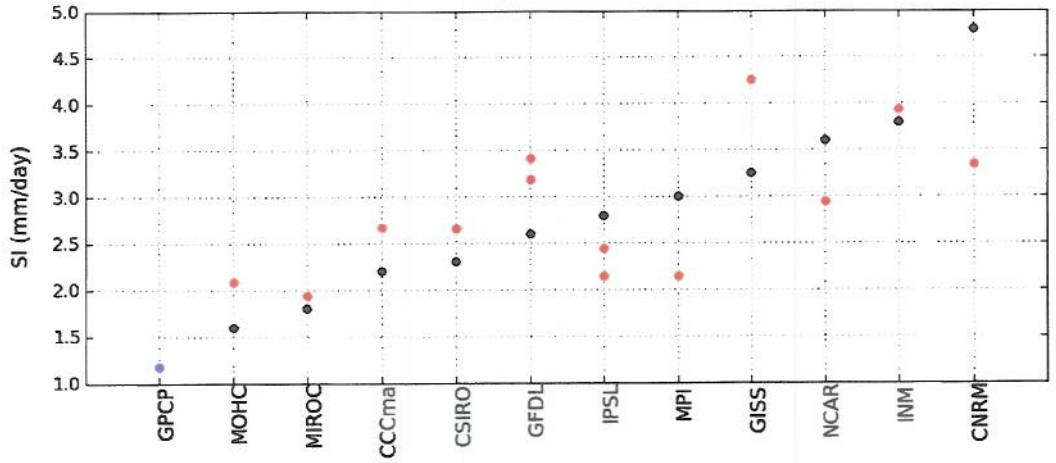

Figure 2: Southern ITCZ index for CMIP5 (red dots) and CMIP3 (balck dots) models (adapted from Bellucci et al., 2010).

which the subseasonal variability is larger in the atmosphere-only model.

2 A first assessment of ENSO in CMIP5

CMIP5 as a multi-model ensemble does not exhibit a quantum leap in ENSO performance or sensitivity, compared to CMIP3 as a multi-model ensemble. Looking at individual modeling centres, about half show an improvement in ENSO amplitude. The multi- model mean state does not exhibit significant changes from CMIP3 to CMIP5, but a slight degradation of surface heat fluxes, although a number of individual centres saw an improvement. Very few models score better for all metrics and most have pluses and minuses. Examination of a selection of physical feedbacks highlights that there is still the potential for the cancellation of errors and that a process-based analysis is fundamental to properly assess ENSO in CGCMs.

The first assessment of basic ENSO properties in control simulations of CMIP5 and a comparison with CMIP3 has been performed. We use the metrics as developed within the CLIVAR Pacific Panel, which assess both the tropical Pacific mean state and interannual properties. We use multi-century pre-industrial simulations for both CMIP3 and CMIP5 as required to ensure statistical robustness. Simulation lengths are 300 years (but for MIROC-ESM-CHEM, 255 years and HadGEM2CC, 240 years). The analysis in Figures 7 and 8 is presented per modelling centre to also assess progress (see Table 1 for official CMIP model names). Precise CMIP5-variables used in the analysis are detailed in the figure captions. Observations or reanalysis used for reference include HadISST1.1 (years 1900-1999), ERA40 (years 1958-2001), CMAP (years 1979-2005) and OAFlux (years 1958-2006 for turbulent and 1984-2006 for radiative).

2.1 ENSO metrics

Under the guidance of the CLIVAR Pacific Panel a set of ENSO metrics has been proposedto facilitate the comparative analysis and understanding of ENSO in CGCMs. These contribute to a wider effort to set up standard metrics for the routine evaluation of CGCMs, as for instance organised for CMIP5. It is key to document the back-

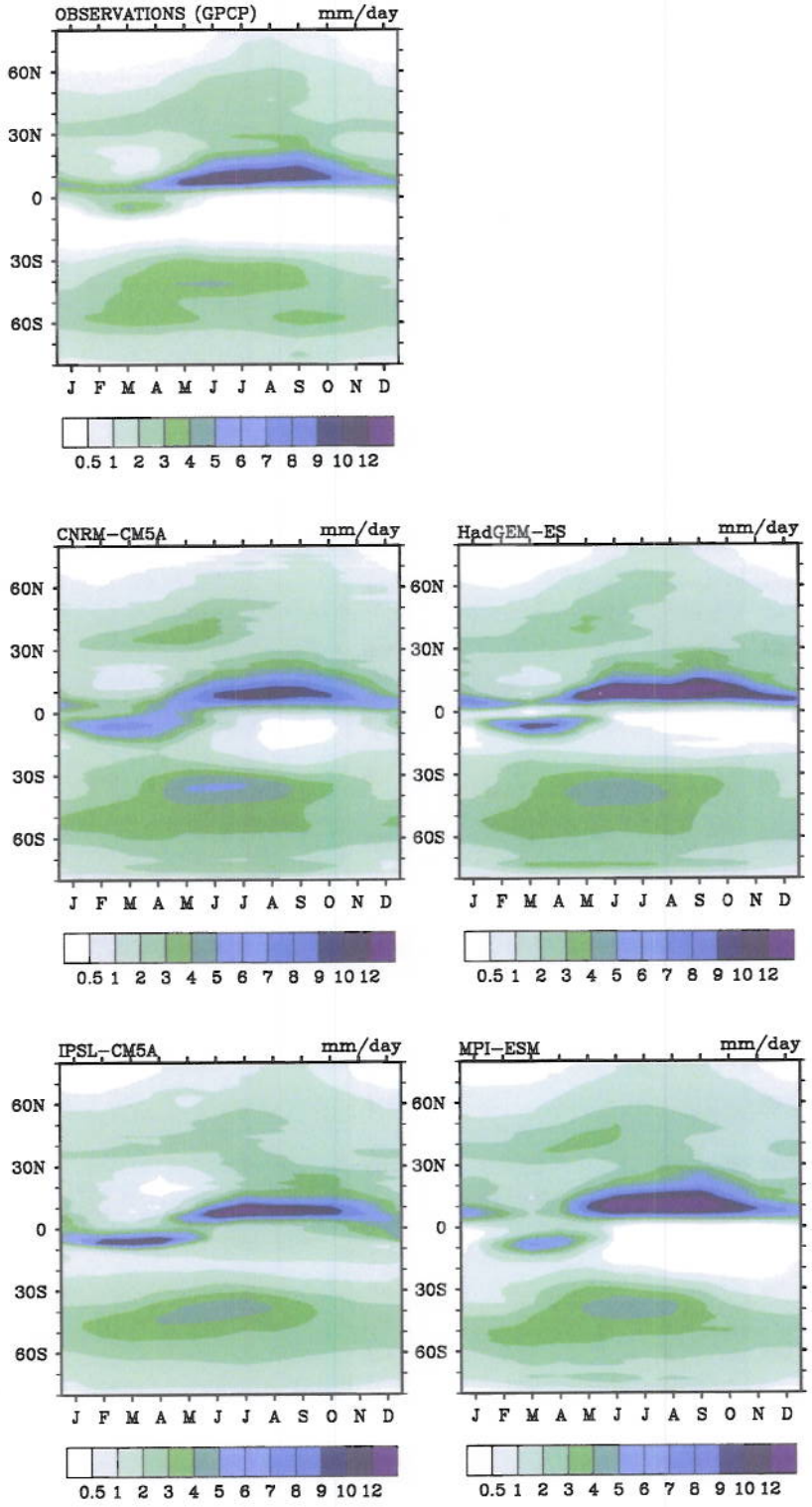

Figure 3: Seasonal cycle of the precipitation in the Eastern Pacific (80W-120W) as observed (GPCP) and simulated by CMIP5 ocean-atmosphere coupled models (CNRM-CM5, HadGEM-ES, IPSL-CM5A, MPI-ESM).

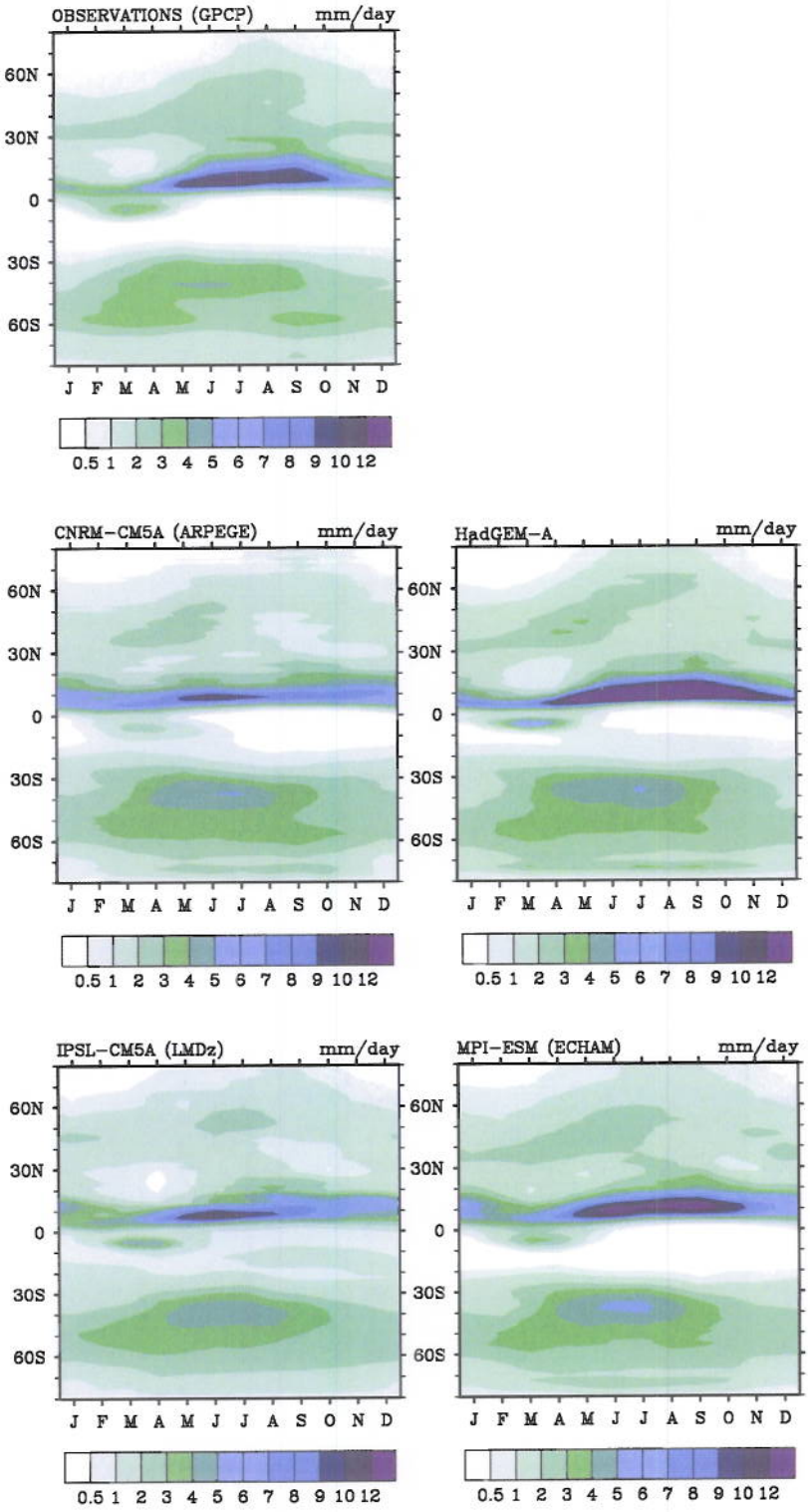

Figure 4: Seasonal cycle of the precipitation in the Eastern Pacific (80W-120W) as observed (GPCP) and simulated by CMIP5 atmosphere-only models (CNRM-CM5, HadGEM-A, IPSL-CM5A, MPI-ESM).

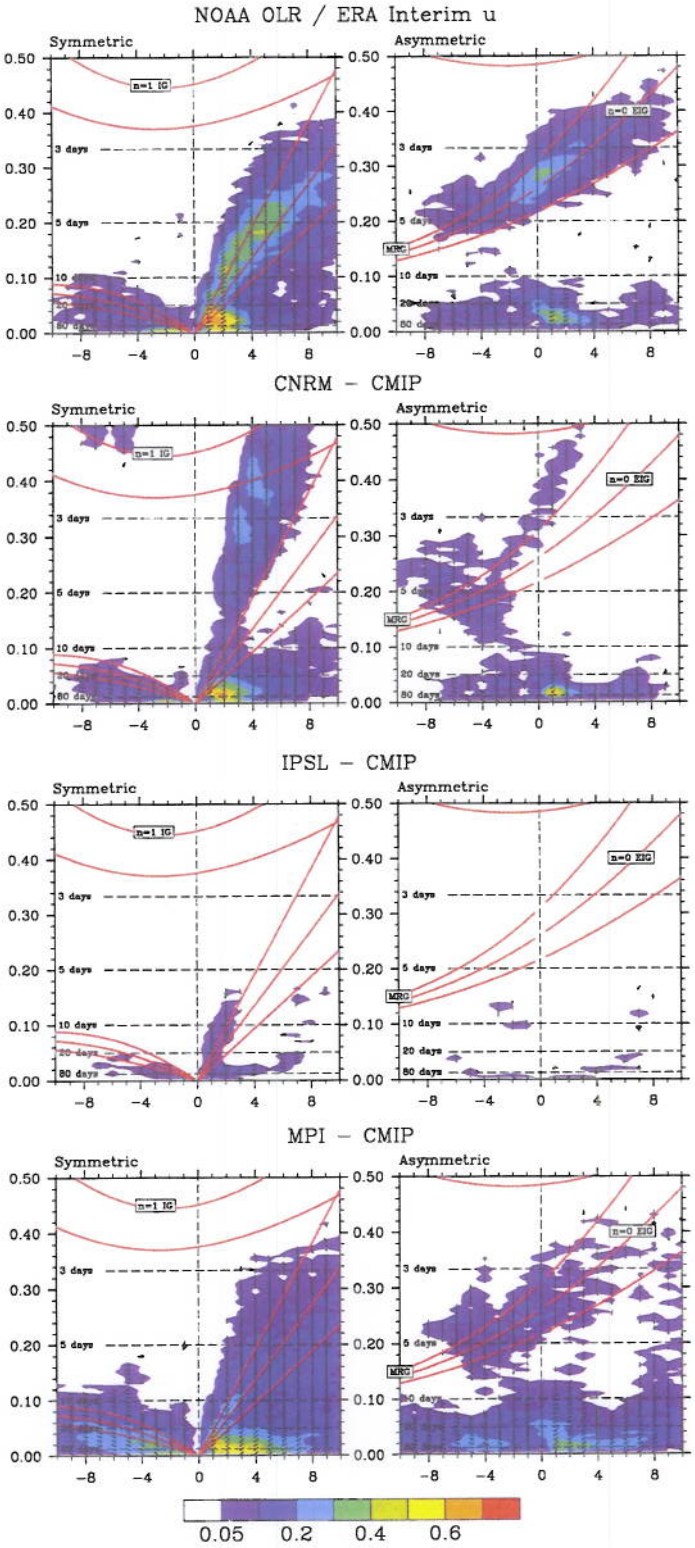

Figure 5: Space and time symmetric and asymmetric spectra of intraseasonal variability as observed (NOAA OLR and ERA Interim) and simulated by the CMIP5 coupled models (CNRM-CM5, IPSL-CM5A, MPI-ESM).

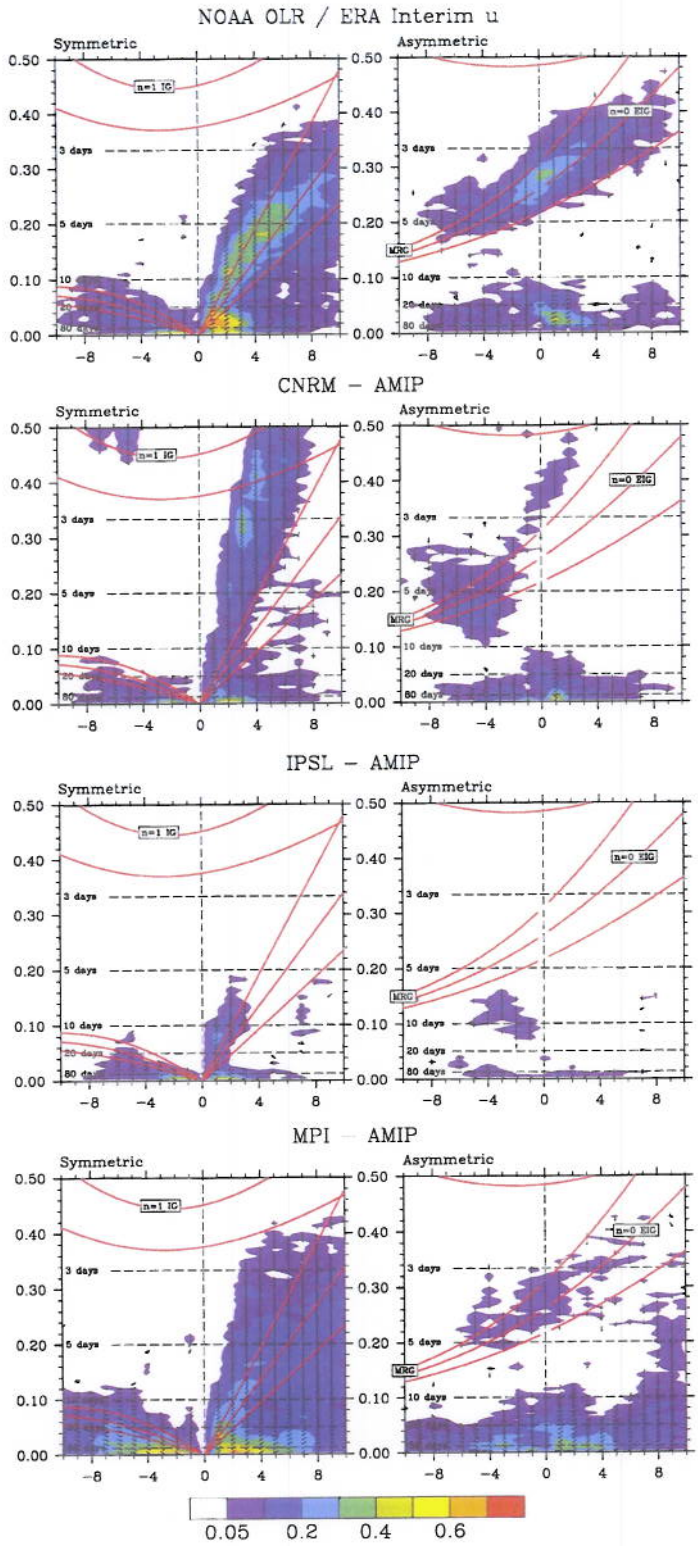

Figure 6: Space and time spectrum of intraseasonal variability as observed (NOAA OLR and ERA Interim) and simulated by the CMIP5 atmosphere-only models (CNRM-CM5, IPSL-CM5A, MPI-ESM).

Modelling centre	CMIP3 model(s)	CMIP5 model(s)
BCC	n/a	BCC-CSM-1
CCCma	CGCM3.1	CanESM2
CNRM	CNRM-CM3	CNRM-CM5
CSIRO	CSIRO-Mk3.0	CSIRO-Mk3.6
GFDL	GFDL2.0	GFDL-ESM2M
	GFDL2.1	
GISS	GISS-AOM	GISS-E2-H
	GISS-EH	GISS-E2-R
	GISS-ER	
IAP	FGOALSg1.0	n/a
INM	INM-CM3.0	INM-CM4
IPSL	IPSL-CM4	IPSL-CM5A-LR
		IPSL-CM5A-MR
MIROC	MIROC3.2-MR	MIROC5
	MIROC3.2-HR	MIROC-ESM
		MIROC-ESM-CHEM
MOHC	HadCM3	HadGEM2-CC
	HadGEM1	HadGEM2-ES
MPI	ECHAM5/MPI-OM	MPI-ESM-LR
MRI	MRI-CGCM2.3.2	MRI-CGCM3
NCC		NorESM1-M

Table 1: CMIP3 and CMIP5 official model names per modelling centre.

ground systematic errors in the tropical Pacific (mean annual cycle and mean state). Indeed, ENSO is defined as an anomaly to these and ENSO errors can often be traced back to these systematic errors. Hence the set of metrics used here include both ENSO and mean state diagnostics (Figure 7). The 4 ENSO metrics encompass ENSO amplitude (Nio3 SST std dev), structure (Nio3 vs Nio4 amplitude), frequency (RMSE of Nio3 SSTA spectra) and heating source (Nio4 precipitation std dev). The other metrics deal with SST, zonal wind stress, precipitation and surface heat flux mean state and annual cycle (Guilyardi and Wittenberg 2010). The specific averaging regions were chosen after correlating different regions to ensure independent metrics are chosen. More details can be found at $http://www.locean-ipsl.upmc.fr/\ ENSO_metrics/index.html$.

2.2 Has ENSO performance in CGCMs improved since CMIP3 ?

2.2.1 ENSO properties

A preliminary analysis of the metrics in Fig 7 first shows that the range of modelled ENSO amplitude in CMIP5 (red dots in Figure 7a) is reduced by about half compared to CMIP3 (blue dots). This is a clear improvement over the CMIP3 ensemble where this diversity was larger than could be explained by observational variability/uncertainty. Although we note that this is a preliminary result as not all modelling groups have submitted output at this stage and the spread of the CMIP5 models could still go up.

The ENSO amplitude, as measured by SST standard deviation, was too large in the central/west Pacific in CMIP3 CGCMs (Nio4 region, 0.8oC compared to 0.65oC in observations) and this has also improved in CMIP5 (0.6oC). Nevertheless there is still the occasional model with spuriously more variability in the west than in the east Pacific (CSIRO-Mk3.6 in CMIP5, CCCma-CGCM3.1 in CMIP3). About half of the centres for which data is available for both CMIP3 and CMIP5 (11 centres) show an improvement in ENSO amplitude while the rest show no change or degradation.

The ENSO spectra metric (Figure 7g) also shows an improved picture in CMIP5 when compared to CMIP3 even at the individual model level. As this metric is sensitive to slight shifts in modelled ENSO spectraand the real-world spectra may not be well constrained by the short observational record this result much be taken with caution. The heating source associated with ENSO, as measured by the Nio4 precipitation standard deviation (Fiure 7d), still exhibits large errors in most CMIP5 models with mixed improvements for individual centres.

2.2.2 Mean state in Tropical Indo-Pacific

The multi-model mean state metrics (Figures 7c,e,f,h,i) do not exhibit significant changes from CMIP3 to CMIP5, but for a slight degradation of surface heat fluxes (Figures 7i), albeit in the presence of significant observational uncertainty in surface fluxes. At the individual level, half of the centres show some improvements, mostly marked for the mean zonal wind stress at the Equator in the Pacific (Figure 7h) while the net surface heat flux in the east Pacific is almost always degraded (Figure7i)

2.2.3 Atmosphere response during ENSO

Several studies point out the central role of the atmosphere general circulation model (GCM) response during ENSO in shaping the modelled ENSO (see for instance Guilyardi al. 2009b and Lloyd et al. 2011). The Bjerknes and heat flux response are computed in Figure 8. There is no qualitative change in the multi-model mean Bjerknes feedback (Figure 8a) although most centres exhibit an improvement in their models. The total heat flux response in Nio3 (Fiure 8b) is improved for a few models (CNRM, MIROC5) although most see a degradation (also seen in the mean heat flux - Figure 7i) leading to more inter-model diversity than in CMIP3. Paradoxically, a number of centres have improved shortwave and latent heat flux response (Figures 8c-d) even though the multi-model mean value does not evolve much. Conversely a number of models have degraded shortwave heat flux response with more models having a positive feedback instead of the observed negative value of -7 Wm-2/C.

While it would have been tempting to conclude from simply looking at the Nio3 anomaly standard deviations (Figure 7a) that the CMIP5 ensemble is converging on reality, examination of these physical feedbacks highlights that there is the potential for the cancellation of errors leading to such convergence. This shows the power of examining these process-based metrics.

With only part of the data available (20 models out of 30-40 planned), CMIP5 as a multi-model ensemble does not exhibit a quantum leap in ENSO performance or sensitivity, compared to CMIP3 as a multi-model ensemble. Looking at individual modeling centres, about half show an improvement in ENSO amplitude. The multi- model mean state does not exhibit significant changes from CMIP3 to CMIP5, but for a slight degradation of surface heat fluxes, although a number of individual centres saw an improvement. Very few models score better for all metrics and most have pluses and minuses. Examination of a selection of physical feedbacks highlights that there is still the potential for the cancellation of errors and that a process-based analysis is fundamental to properly assess ENSO in CGCMs.

We also note that many of the new CGCMs are simulating much more processes than they were in CMIP3 (aerosol indirect effect, strat/trop interactions, land ice, flowing rivers, carbon cycle, ecosystems, and driving by emissions rather than concentrations). This makes things tougher: there are new feedbacks to amplify biases, more uncertain model parameters to constrain and more constraints when finalizing the model set up. But this also holds promise: new avenues for improvement, better contact with observational and theoretical constraints, and new realms of ENSO impacts to be explored.

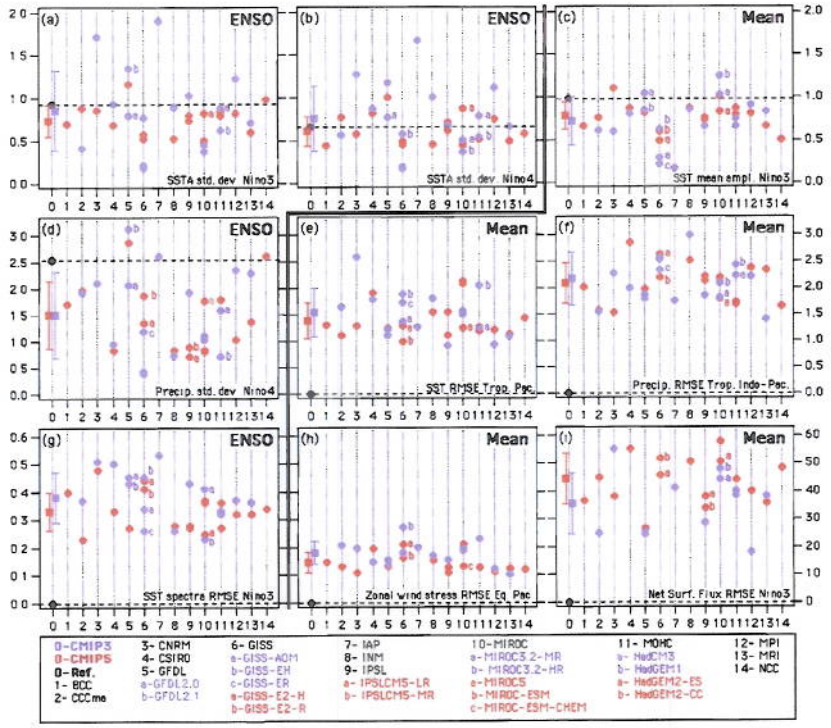

Figure 7: ENSO and mean tropical Pacific metrics for pre-industrial control simulations - CMIP3 (blue) and CMIP5 (red). (a) and (b) SSTA std. dev. in Nio 3 and Nio 4 (C), (c) SST annual cycle amplitude in Nio3, (C), (d) precipitation response (std dev) in Nio4 (mm/day), (e) SST RMS error in tropical Pacific, (C), (f) precipitation spatial RMS error over tropical Indo-Pacific, 30N-30S (mm/day), (g) ENSO power spectrum (Nio3) RMS error, (C2), (h) zonal wind stress spatial RMS error over equatorial Pacific 5N-5S (103Nm2), (i) net surface heat flux RMS error in Nio 3 (Wm2). Reference datasets, shown as black solid circles and dashed lines: HadISST1.1 for (a), (b), (c), (e) and (g); ERA40 for (h); CMAP for (d)(f); OAFlux for (i). The CMIP3 and CMIP5 multi-model mean are shown as squares on the left of each panel with the wiskers representing the model standard deviation. Monthly atmosphere grid CMIP5-variable used: ts for (a), (b), (c), (e) and (g); tauu for ERA40 for (h); pr for (d)(f); hfls (latent), hfss (sensible), rlds (LW down), rlus, (LW up), rsds (SW down), rsus (SW up) to obtain qnet=-hfls-hfss+rlds+rsds-rlus-rsus (i). All fields were interpolated onto a common 1degree grid and then time averaged for mean fields. See metrics $http://www.locean-ipsl.upmc.fr/\ ENSO_metrics/index.html$ for details of computation.

3 European temperature extremes in CMIP5 models

3.1 European temperature extremes in CMIP5/CFMIP2 models

CMIP5 models have difficulties to simulate observed frequencies of extremely hot/cold days. Most of these biases are present in CFMIP2 experiments, and are generally consistent with biases in mean temperatures. In 21^{st} century projections, while the mean European warming tends to increase (decrease) the frequency of hot (cold) days in all models, high uncertainties remain concerning both amplitudes and patterns of these changes. In order to evaluate contributions of large-scale circulation and non-dynamical processes to simulated temperature extremes, we propose a methodology based on a weather-regime approach. While the dynamical contribution to mean biases and changes turns out to be minor, large-scale circulation seems to have a substantial contribution to future uncertainties in winter. In particular the future increase found in CMIP5 in wintertime NAO−, which limits the depletion of cold extremes in Northern Europe, is in noted contradiction with previous CMIP and CFMIP2.

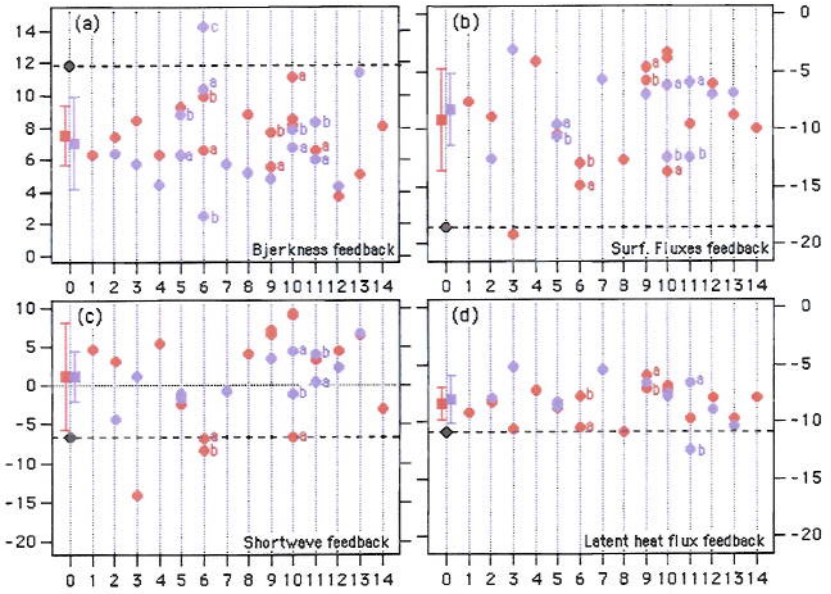

Figure 8: Atmosphere feedbacks during ENSO for pre-industrial control simulations - CMIP3 (blue) and CMIP5 (red). (a) Bjerknes feedback, computed as the regression of Nio 4 wind stress over Nio3 SST (103Nm2/C); (b) heat flux feedback, computed as the regression of total heat flux over SST in Nio3 (Wm- 2/C); (c) Shortwave component of (b); (d) Latent heat flux component of (b). References: ERA40 for (a) and OAFlux for (b), (c) and (d).Monthly atmosphere grid CMIP5-variable used as described in Figures 7. See models and centres legend in Figure 7.

3.1.1 Evaluation in present-day climate

The representation of both summer (JJAS) and winter (DJFM) temperature extremes by 9 CMIP5 / CFMIP2 models, including 4 EUCLIPSE models (CNRM, IPSL, MOHC and MPI), has been evaluated by comparing both *amip* and *historical* runs to E-OBS observations (**?**) over the period 1979–2008. At each point, extremely warm (cold) days are defined as days with a Tmax (Tmin) anomaly above the 90^{th} (below the 10^{th}) centile of the corresponding E-OBS distribution. With this definition, extreme temperatures are said *well represented* if the simulated frequency of extreme days equals 10%.

Figure 9 shows mean frequencies of summertime warm days for all models in *amip* runs. In general, models overestimate hot days in Central Europe (especially MIROC, CNRM) and underestimate them in Scandinavia (esp. CCCMA, MRI) and Western Europe (esp. IPSL, MPI). Figure 10 is similar but for wintertime cold days, showing a general understimation of cold extremes in Scandinavia and South-Western Europe (except CNRM and MOHC) and an overestimation over North-Eastern Europe (except MPI and MRI). These biases are quasi-systematically amplified in *historical* runs, but with same spatial patterns. They often scale with mean biases, except in a few cases: for instance IPSL's summer cold bias is weak over Western Europe despite a high underestimation of hot extremes.

3.1.2 Future changes and uncertainties

Future changes in extreme temperatures are assessed by considering for each model the mean frequency, in the *rcp85* run over 2070–2099, to exceed the 90^{th} or 10^{th} centile of the *historical* run over 1979–2008. Given the mean European warming in climate change scenarios, the frequency of summertime warm extremes is projected to increase

from 10% in recent period (by definition) to ~50% by late 21^st century, with a large model spread (25% for MRI, 80% for IPSL). A meridional gradient is found in the model-ensemble response, with a higher (lower) increase in warm extremes in Southern (Northern) Europe. In winter, the frequency of cold extremes is projected to decrease from 10% to ~1%, again with a large model spread (0.3% for IPSL and MIROC, 2.5% for NCC). This depletion is generally higher in North-Eastern Europe. Patterns of changes in both summertime and wintertime extremes are consistent with mean temperature changes, but not necessarily scaled in amplitude: for instance the highest mean warming in summer occurs for CCCMA while the highest increase in hot extremes occurs for IPSL.

A similar diagnostic was made in CFMIP2 experiments by comparing *amipFuture* to *amip* run (only EUCLIPSE models available). Despite similarities in the main responses (increase in warm extremes, decrease in cold extremes), patterns and amplitude differ from CMIP5 experiments, which is likely due to the difference in SSTs. We therefore believe that an extra CFMIP2 experiment forced, for each model, by the native SST anomaly derived from the *rcp85* run could be helpful.

3.1.3 Separating dynamical vs. non-dynamical contributions

European temperatures are mainly driven by the North-Atlantic atmospheric dynamics. The attribution of both present-day biases and future changes to dynamical (i.e. large-scale circulation) and/or other processes (i.e. radiative fluxes, soil or cloud feedbacks) is therefore a key question. In order to separate the role of large-scale circulation we use a weather-regime approach that clusters daily anomalies of Z500 into preferred states. Regimes derived from NCEP2 reanalysis (?) are taken as reference. We find 4 quasi-equiprobable regimes for both summer (Atlantic Low, Blocking, Atlantic Ridge and NAO−, see ?) and winter (NAO+, NAO−, Blocking and Atlantic Ridge, see ?), which can be described by their frequencies of occurrence f_k and their intra-class distributions of circulations d_k (or structures). Any mean variable $\overline{X}$ (e.g., frequency of extreme days) can be written as:

$$\overline{X} = \sum_k f_k \cdot \Phi(d_k)$$

with Φ a transfer function between circulations and X. Thus a difference between two values of $\overline{X}$ (e.g., model vs. observations or future F vs. present P) can be broken down into:

$$\Delta^{F-P}\overline{X} = \underbrace{\sum_k \Delta f_k \cdot \Phi^P(d_k^P)}_{BC} + \underbrace{\sum_k f_k^P \cdot \Phi^P(\Delta d_k)}_{WCd} + \underbrace{\sum_k f_k^P \cdot \Delta\Phi(d_k^F)}_{WC\Phi} + \epsilon$$

where $BC + WCd$ is the dynamical contribution (differences in regimes' frequencies + structures) and $WC\Phi$ the non-dynamical contribution (see details in ?).

Figure 11 shows biases and future changes in regimes' frequencies for both seasons. Present-day biases are contrasted, except for the winter Blocking which is underestimated by all models (a,c). As in previous CMIP, a robust increase in summer Blocking is found (b). Surprisingly, CMIP5 models exhibit an increase in winter NAO− to the detriment of NAO+ and Blocking (d), which is in noted contradiction with increases in NAO+ found in all previous CMIP and in CFMIP2 experiments (*amipFuture* vs. *amip* frequencies). Biases/changes in regimes' structures are assessed through a flow-analogue approach as in ?. Eventually, applying the linear breakdown methodology to mean frequencies of warm/cold extremes in the model-ensemble shows that:

- dynamical contributions to present-day biases and future changes are minor, especially in summer. The under-

estimation of wintertime Blocking slightly contributes to the lack of cold extremes in Central Europe, while the future increase in wintertime NAO− tends to limit the depletion in cold extremes in Scandinavia.

- dynamical contributions to uncertainties (model-spread) are minor in summer, but substantial in winter, especially due to disagreements on changes in Atlantic Ridge frequency and NAO−/Blocking structures (Figure 12).

The next step will consist in understanding non-dynamical contributions, which seem to play a major role, especially in summer. In particular, contributions of radiative fluxes and potential roles of land surface and cloud feedbacks to present-day biases and future uncertainties in temperature extremes will be investigated.

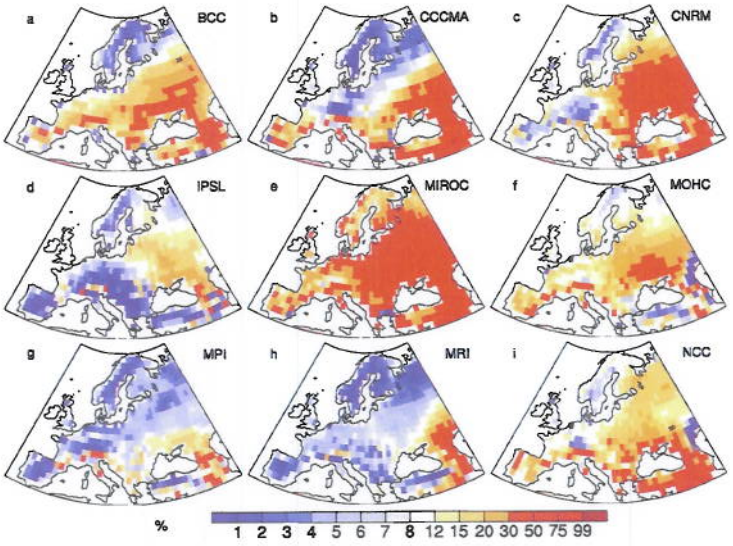

Figure 9: Frequencies of summertime extremely hot days in *amip* experiments.

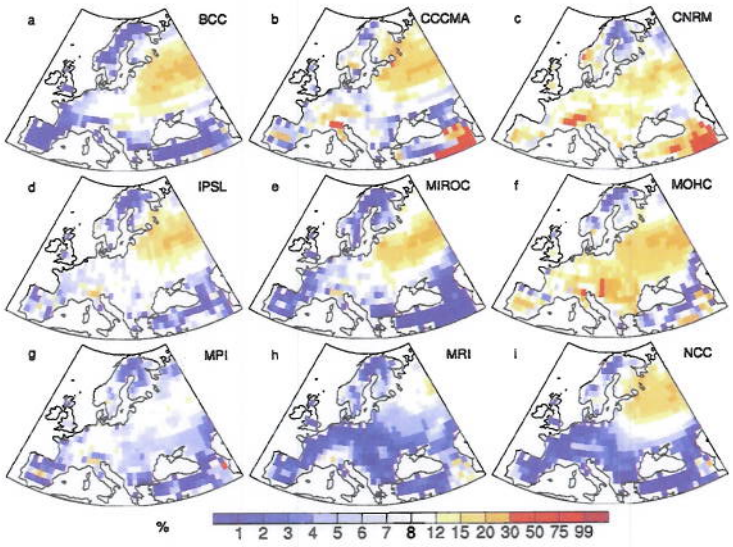

Figure 10: Frequencies of wintertime extremely cold days in *amip* experiments.

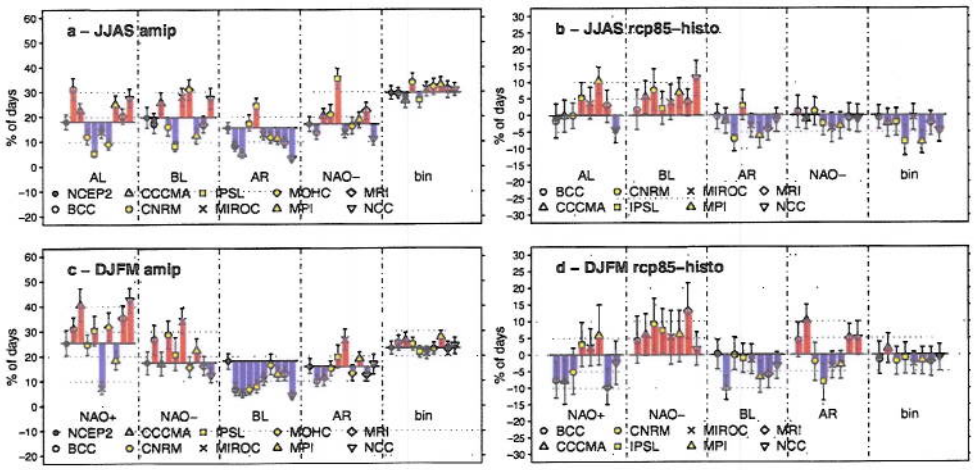

Figure 11: Frequencies of occurrence of weather regimes. (a–b) Summer: (a) *amip* frequencies as departures from NCEP2 reference and (b) *rcp85−historical* differences. (c–d) Same for winter. EUCLIPSE models are highlighted in yellow. MOHC is missing in right panels (Z500 unavailable so far).

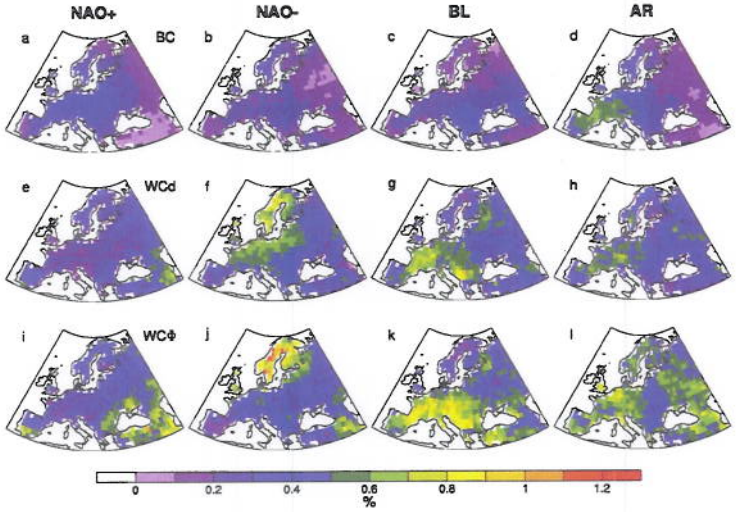

Figure 12: Breaking-down methodology applied to future uncertainties in wintertime cold extremes: multi-model standard deviations of each term of the equation, sorted by regime (columns) and contribution type (rows).

4 References

- Bellucci, A., S. Gualdi, A. Navarra (2010), The Double-ITCZ Syndrome in Coupled General Circulation Models: The Role of Large-Scale Vertical Circulation Regimes. J. Climate, 23, 1127-1145.
- Cassou, C. (2008), Intraseasonal interaction between the Madden-Julian Oscillation and the North Atlantic Oscillation, Nature, 455 (7212), pp. 523-527. doi: 10.1038/nature07286.
- Cassou, C., L. Terray, and A.S. Phillips (2005), Tropical Atlantic Influence on European Heat Waves, J. Climate, 18 (15), pp. 2805-2811.

- Cattiaux, J., P. Yiou, and R. Vautard (2011a), Dynamics of future seasonal temperature trends and extremes in Europe: a multi-model analysis from CMIP3, Climate Dynamics, published online. doi:10.1007/s00382-011-1211-1.
- Cattiaux, J., H. Douville, A. Ribes, F. Chauvin, and C. Plante (2011b), Towards a better understanding of wintertime cold extremes over Europe: A pilot study with CNRM and IPSL atmospheric models, Clim. Dynamics, submitted.
- Dai, A. (2006), Precipitation Characteristics in Eighteen Coupled Climate Models. J. Climate, 19, 4605-4630.
- de Szoeke, Simon P., Shang-Ping Xie (2008), The Tropical Eastern Pacific Seasonal Cycle: Assessment of Errors and Mechanisms in IPCC AR4 Coupled Ocean-Atmosphere General Circulation Models. J. Climate, 21, 257-2590.
- Guilyardi E., P. Braconnot, F.-F. Jin, S. T. Kim, M. Kolasinski, T. Li and I. Musat (2009b), Atmosphere feedbacks during ENSO in a coupled GCM with a modified atmospheric convection scheme. J. Climate, 22, 5698-5718
- Guilyardi E. and A. Wittenberg (2010), ENSO and tropical Pacific metrics for CMIP5. IPCC Expert meeting on Assessing and Combining Multi Model Climate Projections, Boulder, USA, January 2010
- Haylock, M.R. et al. (2008), A European daily high-resolution gridded data set of surface temperature and precipitation for 1950-2006, J. Geophys. Res., 113, pp. 20119. doi: 10.1029/2008JD10201.
- Kanamitsu, M. et al. (2002), NCEP-DOE AMIP-II Reanalysis (R-2), Bull. Amer. Meteorol. Soc., 83 (11), pp. 1631-1643.
- Lin, Jia-Lin (2007), The Double-ITCZ Problem in IPCC AR4 Coupled GCMs: Ocean-Atmosphere Feedback Analysis. J. Climate, 20, 4497-4525.
- Lin, Jia-Lin, and Coauthors (2006), Tropical Intraseasonal Variability in 14 IPCC AR4 Climate Models. Part I: Convective Signals. J. Climate, 19, 2665-2690.
- Lloyd, J., E. Guilyardi and H. Weller (2011), The role of atmosphere feedbacks during ENSO in the CMIP3 models, Part II: using AMIP runs to understand the heat flux feedback mechanisms, Clim. Dynamics, 37, 1271-1292, DOI: 10.1007/s00382-010-0895
- Lloyd J., E. Guilyardi, H. Weller (2012), The Role of Atmosphere Feedbacks during ENSO in the CMIP3 Models. Part III: The Shortwave Flux Feedback. J. Climate, in press
- Wheeler, Matthew, George N. Kiladis (1999), Convectively Coupled Equatorial Waves: Analysis of Clouds and Temperature in the Wavenumber-Frequency Domain. J. Atmos. Sci., 56, 374-399.